# Supplementary Materials: Radiomic Based Machine Learning Performance for a Three Class Problem in Neuro-Oncology: Time to Test the Waters?

**Sarv Priya, Yanan Liu, Caitlin Ward, Nam H. Le, Neetu Soni, Ravishankar Pillenahalli Maheshwarappa, Varun Monga, Honghai Zhang, Milan Sonka and Girish Bathla**

**Text S1**

## 1. Patient Selection

This was a retrospective study approved by the local institutional review board (IRB-ID 201912239). Between 2010–2019, patients above the age of 18 years were identified using a combination of electronic medical records and institutional cancer registries. Since lung and breast cancer account for most of the cases of brain metastases, the metastatic lesion cohort was confined to patients with a known lung or breast primary. Eligibility criteria included: preoperative MRI scans that had all multiparametric (axial T1W, T2W, FLAIR, ADC and T1 contrast enhanced (CE)) sequences available, presence of a contrast enhancing tumor, and no prior history of treatment, biopsy or surgical resection. Patients with non-enhancing tumors and motion artifact were excluded. A total of 253 patients were included in the study (metastatic ($n$ = 120, 47.4%), PCNSL ($n$ = 40, 15.8%), and GBM ($n$ = 93, 36.8%)).

## 2. MRI Imaging Parameters

### *2.1. MRI Scanning Parameters for Siemens 1.5 T MRI (Siemens, Erlangen, Germany)*

T1W (TR/TE/TI: 1950/10/840, NEX: 2, slice thickness: 5 mm, matrix: 320 × 256, field of view 240 mm, pixel size 0.75 mm)

T2W (TR/TE: 4000/90, NEX: 2, slice thickness: 5 mm, matrix: 512 × 408, field of view 240 mm, pixel size 0.5 mm);

FLAIR (TR/TE/TI: 9000/105/2500, NEX: 1, slice thickness: 5 mm, matrix: 384 × 308, field of view 240 mm, pixel size 0.6 mm)

DWI (TR/TE: 4000/74, NEX: 3, slice thickness: 5 mm, matrix: 128 × 128, field of view 240 mm, pixel size 1.8 mm)

T1W-CE (TR/TE/TI: 570/13, NEX: 2, slice thickness: 5 mm, matrix: 384 × 312, field of view 240 mm, pixel size 0.62 mm)

T1W-CE images were acquired 2–3 minutes after administration of gadobenate dimeglumine (Multihance; Bayer Healthcare Pharma) or gadobutrol (Gadavist; Bayer Healthcare Pharma, Berlin, Germany) injected at the rate of 0.1 mL/kg body weight.

### *2.2. MRI Scanning Parameters for Siemens 3 T MRI (Siemens, Erlangen, Germany)*

T1W (TR/TE/TI: 2000/11/899, NEX: 1, slice thickness: 5 mm, matrix: 384 × 312, field of view 240 mm, pixel size 0.62 mm)

T2W (TR/TE: 4000/105, NEX: 2, slice thickness: 5 mm, matrix: 448 × 364, field of view 240 mm, pixel size 0.5 mm)

FLAIR (TR/TE/TI: 9000/108/2500, NEX: 1, slice thickness: 5 mm, matrix: 384 × 312, field of view 240 mm, pixel size 0.62 mm)

DWI (TR/TE: 4250/64, NEX: 1, slice thickness: 5 mm, matrix: 160 × 160, field of view 240 mm, pixel size 1.5 mm)

T1W-CE (TR/TE/TI: 2000/12/900, NEX: 1, slice thickness: 5 mm, matrix: 384 × 312, field of view 240 mm, pixel size 0.62 mm)

**3. Image Preprocessing Was Performed as per International Biomarker Standardization Initiative (IBSI) Guidelines with Following Steps Performed:**

**Resampling—Registration—Normalization—Segmentation—Feature Extraction—Model Building**

**Image Preprocessing:**

1. Image format conversion: DICOM images were converted to NIfTI
2. Image resampling: To standardize MR image resolution, all MR image volumes were resampled to 1 × 1 × 5 $mm^3$ voxel size using the AFNI package (https://afni.nimh.nih.gov/).
3. Co-registration: Images acquired during the same scanning session were mutually registered to T1 W sequence using Advanced Normalization Tools (ANTs) (http://stnava.github.io/ANTs/).
4. Intensity normalization: Image intensities were normalized to [0,255] using the feature scaling method available in the ANTs registration suite (http://stnava.github.io/ANTs/).

**4. Tumor Segmentation**

1. Highly accurate 3D segmentation was performed on axial T1-CE and FLAIR images by a semi-automated approach using LOGISMOS (Layered Optimal Graph Image Segmentation for Multiple Objects and Surfaces) software. After the automated LOGISMOS graph segmentation, the next step allows the expert observer to efficiently fix small localized segmentation inaccuracies by interacting with the LOGISMOS optimization algorithm instead of redrawing surfaces on all affected 2D slices. As such, only a few additional expert-identified points indicating correct surface locations are typically needed to modify the 3D surfaces and thus correct the 3D segmentations in their entirety.
2. Region of interests/masks generation- Four different region of interests (masks) were created using T1-CE and FLAIR images: i) whole tumor (enhancing plus necrotic); ii) enhancing only; iii) necrotic only; and iv) peritumoral edema. The first three masks were created from the T1-CE images by first generating masks for the whole tumor (encompassing both enhancing and necrotic segments) and necrotic components and then subtracting the necrotic mask from whole tumor to generate enhancing mask. The FLAIR images were used to generate a mask for the entire lesion (whole tumor and surrounding edema). Edema mask was eventually obtained by subtracting T1-CE derived whole tumor mask from the FLAIR mask (Figure S1).

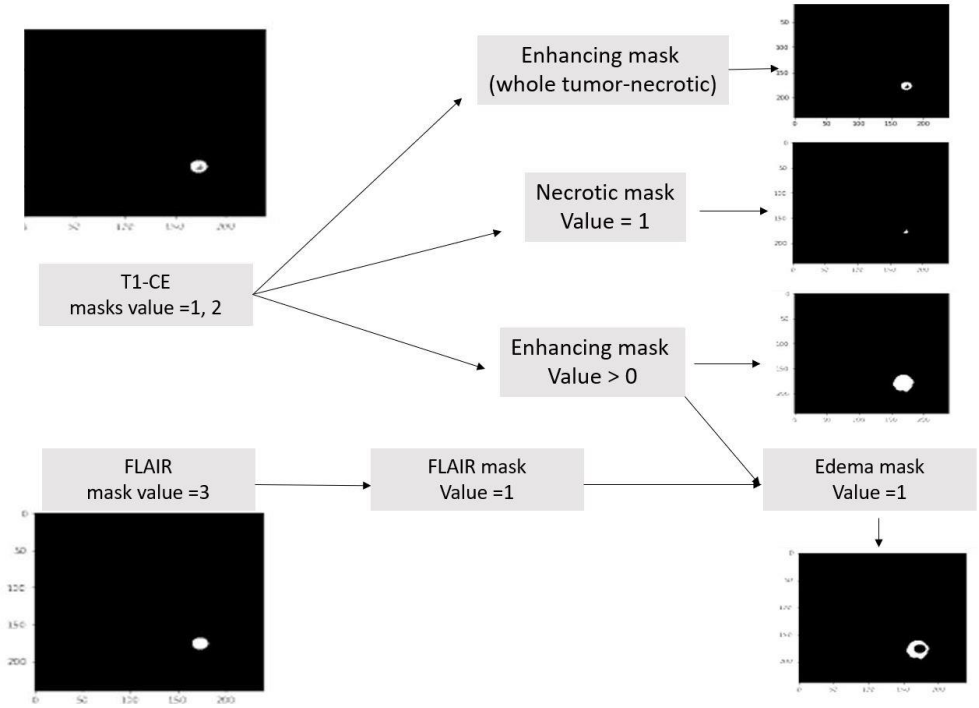


**Figure S1.** Block diagram showing mask separation. The left two masks were the masks segmented using LOGISMOS software. Different masks had different values because we used Logismos software to segment out the masks. In order to separate different masks, the software assigned different masks different value. The right 4 figures were separated masks: all the masks value equals 1 and background equals 0. We used the right separated masks to extract radiomic features.

## 5. Texture Feature Extraction

1. A total of 107 features were extracted using Pyradiomics 3.0:3D shape features ($n$ = 14), first order features ($n$ = 18), gray level co-occurrence matrix features ($n$ = 24), gray level dependency matrix features ($n$ = 14), gray level run length matrix features ($n$ = 16), gray level size zone matrix features ($n$ = 16) and neighboring gray tone difference matrix features ($n$ = 5).
2. The default value for the number of bins was fixed by bin width of 25 gray levels. In rare cases where the edema or necrosis were minimal, leading to absence of a corresponding mask, the value of the corresponding feature was set to −9999.

**Table S1.** Least axis length masks.

| Patient | Edema Mask (3D Shape) | Whole Tumor Mask (3D Shape) | Enhancing Mask (3D Shape) | Necrotic Mask (3D Shape) |
|---|---|---|---|---|
| Patient Number | Least Axis Length (mm) | Least Axis Length (mm) | Least Axis Length (mm) | Least Axis Length (mm) |
| 1 | 18.7 | 27.2 | 27.2 | −10,000 |
| 2 | 25.5 | 15.4 | 15.4 | −10,000 |
| 3 | 81.8 | 33.9 | 32.8 | 16.5 |
| 4 | 28.8 | 16.5 | 15.3 | 8.87 |
| 5 | 23.7 | 13.1 | 12.8 | 0 |
| 6 | 25.4 | 9.23 | 9.23 | −10,000 |
| 7 | 17.6 | 11 | 11 | −10,000 |
| 8 | 39.3 | 33.2 | 30.6 | 21.9 |
| 9 | 58.1 | 19.2 | 18.8 | 9.05 |
| 10 | 35.9 | 19.8 | 19.4 | 6.17 |
| 11 | 19.6 | 9.93 | 9.94 | 0 |
| 12 | −10,000 | −10,000 | −10,000 | −10,000 |
| 13 | 8.26 | 8.22 | 8.22 | −10,000 |

| | | | | |
|---|---|---|---|---|
| 14 | 46.4 | 25.4 | 25.4 | −10,000 |
| 15 | 57.5 | 28.1 | 28 | 7.59 |
| 16 | 37 | 23.5 | 23.5 | −10,000 |
| 17 | 35.7 | 21.2 | 21.2 | −10,000 |
| 18 | 45.2 | 8.84 | 34.2 | 32.7 |
| 19 | 12.5 | −10,000 | 6.99 | 6.99 |
| 20 | 33.4 | 8.4 | 9.57 | 0 |
| 21 | 9.41 | 8.85 | 8.85 | −10,000 |
| 22 | 47 | 18.2 | 18 | 3.97 |
| 23 | 23.9 | 15 | 15 | −10,000 |
| 24 | 5.61 | 0 | 0 | −10,000 |
| 25 | 10.3 | 9.24 | 8.88 | 0 |
| 26 | 17.2 | 13.3 | 12.4 | 6.54 |
| 27 | 55.6 | 17.2 | 20.8 | 17.7 |
| 28 | 31.7 | 19.3 | 19.3 | −10,000 |
| 29 | 48.5 | 20.1 | 19.6 | 6.27 |
| 30 | 27.8 | 23.1 | 20.4 | 13.9 |
| 31 | 36.9 | 48.3 | 47.2 | 23 |
| 32 | 51.6 | 39.3 | 38.2 | 15.3 |
| 33 | 67.6 | 29.9 | 29.3 | 11.3 |
| 34 | 52.2 | 38.1 | 37.7 | 23.7 |
| 35 | 42.2 | 25.2 | 23.9 | 11.3 |
| 36 | 42 | 57 | 51 | 32.1 |
| 37 | 50.7 | 37.3 | 34.1 | 22.6 |
| 38 | 46.8 | 28.3 | 26.8 | 17.1 |
| 39 | 43.3 | 54.8 | 51.1 | 28.1 |
| 40 | 48.1 | 21.5 | 21 | 9.78 |
| 41 | 60.4 | 35.6 | 34.2 | 22.8 |
| 42 | 61 | 37.4 | 35.7 | 15.8 |
| 43 | 50.4 | 47 | 40.7 | 30.8 |
| 44 | 36.7 | 34 | 31.6 | 20.3 |
| 45 | 71.5 | 31 | 30.4 | 15.1 |
| 46 | 57.5 | 44.1 | 39.8 | 23.4 |
| 47 | 45.3 | 29.8 | 27.6 | 17.4 |
| 48 | 57.5 | 37.4 | 34.5 | 24.5 |
| 49 | 16.3 | 11.2 | 10.9 | 5.31 |
| 50 | 26.7 | 28 | 26.9 | 9.28 |
| 51 | 33.3 | 23.4 | 22.3 | 11.5 |
| 52 | 49.2 | 45.9 | 42.4 | 21.6 |
| 53 | 40.7 | 45.2 | 41.3 | 25.1 |
| 54 | 40.8 | 30.8 | 29.1 | 11 |
| 55 | 37.9 | 12.7 | 12.6 | 0 |
| 56 | 38.1 | 15.2 | 14.8 | 5 |
| 57 | 34.9 | 26 | 24.3 | 12 |
| 58 | 52.4 | 45.4 | 44.8 | 14 |
| 59 | 56.9 | 29.8 | 28.5 | 16.7 |
| 60 | 63.8 | 38.6 | 36.6 | 21.4 |
| 61 | 50.8 | 24.9 | 25.8 | 10.9 |
| 62 | 38.9 | 29.4 | 28.8 | 11.5 |
| 63 | 38.3 | 21.7 | 20.6 | 11.1 |
| 64 | 61 | 29.4 | 28.5 | 11.5 |
| 65 | 55.9 | 24.8 | 24.2 | 11.2 |
| 66 | 63.2 | 31.6 | 32.1 | 17.1 |
| 67 | 40.1 | 24.2 | 22.2 | 14.4 |
| 68 | 46 | 24.8 | 23.6 | 13.1 |
| 69 | 58.3 | 25.1 | 24.1 | 10.3 |

| | | | | |
|---|---|---|---|---|
| 70 | 44.5 | 21 | 20.1 | 10.5 |
| 71 | 50.7 | 37.5 | 35.9 | 19.2 |
| 72 | 25.6 | 21.3 | 21.2 | 3.74 |
| 73 | 46.7 | 28.3 | 26.3 | 16.3 |
| 74 | 46 | 35.2 | 34.9 | 27.4 |
| 75 | 49.1 | 42.4 | 38.3 | 26.5 |
| 76 | 45.9 | 41 | 36.7 | 28.1 |
| 77 | 56.8 | 29.6 | 28.3 | 20.7 |
| 78 | 49.9 | 27.1 | 26 | 13.6 |
| 79 | 52.1 | 34.3 | 34.3 | −10,000 |
| 80 | 45.6 | 41.8 | 41.8 | 6.37 |
| 81 | 40.6 | 36.7 | 35.9 | 25 |
| 82 | 39.6 | 44.9 | 43.2 | 18.5 |
| 83 | 61.9 | 35 | 32.8 | 19.6 |
| 84 | 49.3 | 34.4 | 32.7 | 17.6 |
| 85 | 41.2 | 30.2 | 27 | 17.9 |
| 86 | 41.6 | 27.9 | 27.4 | 8.16 |
| 87 | 50.2 | 39.2 | 35.9 | 19.7 |
| 88 | 48.1 | 32.7 | 30.5 | 25.8 |
| 89 | 55.2 | 45.1 | 42.9 | 20.1 |
| 90 | 35.7 | 36.1 | 35 | 20.4 |
| 91 | 22.1 | 15.8 | 14.9 | 8.96 |
| 92 | 24.8 | 22.7 | 21.4 | 10.3 |
| 93 | 54.6 | 35.8 | 35.6 | 7.23 |
| 94 | 46.7 | 34.5 | 32.7 | 19.1 |
| 95 | 40 | 37.1 | 35.8 | 15.6 |
| 96 | 27.3 | 16 | 15.3 | 6.86 |
| 97 | 23.4 | 19.7 | 19.7 | −10,000 |
| 98 | 48.1 | 24.6 | 23.7 | 12.3 |
| 99 | 45.2 | 29.7 | 27.4 | 13.6 |
| 100 | 58.1 | 49 | 48.8 | 5.21 |
| 101 | 54 | 40.6 | 38.6 | 22.8 |
| 102 | 32.3 | 25.3 | 23.8 | 11.8 |
| 103 | 59 | 38 | 37.7 | 8.8 |
| 104 | 22 | 20.9 | 20.5 | 5.96 |
| 105 | 48.8 | 23.4 | 22.1 | 13.4 |
| 106 | 50.8 | 30.6 | 30.1 | 10.1 |
| 107 | 48 | 38.5 | 36.7 | 20.5 |
| 108 | 36.5 | 28 | 26 | 15.8 |
| 109 | 39.5 | 29.7 | 28.4 | 19.8 |
| 110 | 22.5 | 14.3 | 13.5 | 0 |
| 111 | 38.8 | 20.9 | 20.6 | 6.49 |
| 112 | 33 | 34.8 | 33.7 | 13.7 |
| 113 | 44 | 36.5 | 33 | 22.6 |
| 114 | 36.9 | 34.5 | 34.4 | 5.03 |
| 115 | 50.5 | 50.7 | 48.2 | 26.4 |
| 116 | 30.5 | 19.1 | 18.3 | 8.67 |
| 117 | 48.2 | 41.6 | 37.4 | 26.4 |
| 118 | 50.6 | 41.2 | 37.9 | 25.5 |
| 119 | 41.4 | 38.2 | 37.1 | 15.8 |
| 120 | 80.8 | 49.1 | 49.4 | 22.5 |
| 121 | 43 | 43.9 | 44 | 14.6 |
| 122 | 38.1 | 17.7 | 17.3 | 5.86 |
| 123 | 31.7 | 17.8 | 17.8 | −10,000 |
| 124 | 11.6 | 15.3 | 14.2 | 6.31 |
| 125 | 19.5 | 14.3 | 12.9 | 7.54 |

| | | | | |
|---|---|---|---|---|
| 126 | 9.25 | 0 | 0 | −10,000 |
| 127 | 30.1 | 18.6 | 17.2 | 8.38 |
| 128 | 16.5 | 9.5 | 9.5 | −10,000 |
| 129 | 26.9 | 12 | 11.7 | 0 |
| 130 | 17 | 0 | 0 | −10,000 |
| 131 | 0 | 5.81 | 5.81 | −10,000 |
| 132 | 50.2 | 13.5 | 13.5 | −10,000 |
| 133 | 24.7 | 22.3 | 20.4 | 10.8 |
| 134 | 44.8 | 24.2 | 24.2 | −10,000 |
| 135 | 24.8 | 12.1 | 12.1 | −10,000 |
| 136 | 37.6 | 9.33 | 9.51 | 0 |
| 137 | 11.9 | 6.18 | 6.18 | −10,000 |
| 138 | 15.6 | 15.2 | 14.6 | 8.2 |
| 139 | 0 | 0 | 0 | −10,000 |
| 140 | 35.5 | 13.9 | 13.7 | 0 |
| 141 | 38.8 | 13.1 | 12.8 | 0 |
| 142 | 32.6 | 10.9 | 10.6 | 0 |
| 143 | 52.9 | 16.1 | 15.6 | 6.06 |
| 144 | 12.8 | 0 | 0 | −10,000 |
| 145 | 13.9 | 10.2 | 10.2 | −10,000 |
| 146 | 43.4 | 7.87 | 24.3 | 21.2 |
| 147 | 9.58 | 6.99 | 6.99 | −10,000 |
| 148 | 35.7 | 16.6 | 16.2 | 5.36 |
| 149 | 48.7 | 18.1 | 16.9 | 9.81 |
| 150 | 36.7 | 16.6 | 15.2 | 9.54 |
| 151 | 36.4 | 7 | 19.1 | 19.4 |
| 152 | 27.3 | 16.4 | 16.4 | −10,000 |
| 153 | 25 | 11.8 | 11.8 | −10,000 |
| 154 | 25.2 | 10.3 | 10.3 | −10,000 |
| 155 | 37.2 | 23.9 | 22.4 | 11.6 |
| 156 | 18.4 | 9.79 | 9.51 | 4.24 |
| 157 | 34.3 | 28.2 | 28 | 4.79 |
| 158 | 47.3 | 17.1 | 16.5 | 8.15 |
| 159 | 30.7 | 23.8 | 21.8 | 15 |
| 160 | 42.3 | 18.7 | 18.1 | 5.49 |
| 161 | 29.5 | 12.8 | 12.2 | 5.57 |
| 162 | 7.92 | 9.29 | 9.29 | −10,000 |
| 163 | 37.3 | 14.3 | 14 | 0 |
| 164 | 54.8 | 13 | 12.9 | 0 |
| 165 | 51.9 | 22 | 22 | −10,000 |
| 166 | 32.2 | 14.8 | 19.8 | 12 |
| 167 | 79.1 | 20.4 | 20.3 | 5.3 |
| 168 | 49.1 | 22.8 | 33.6 | 32.2 |
| 169 | 23.2 | 21.5 | 20.5 | 10.5 |
| 170 | 26.9 | 17.3 | 16.6 | 7.78 |
| 171 | 15 | 5.93 | 5.93 | −10,000 |
| 172 | 37.7 | 8.88 | 8.69 | 0 |
| 173 | 3.89 | 9.1 | 8.82 | 2.91 |
| 174 | 42 | 17.6 | 16.5 | 8.87 |
| 175 | 80.9 | 31.3 | 29.6 | 13 |
| 176 | 13.9 | 11.4 | 11.4 | −10,000 |
| 177 | 15.6 | 13.8 | 13.5 | 0 |
| 178 | 32.7 | 22.1 | 22.1 | −10,000 |
| 179 | 33.9 | 21.9 | 21.8 | 4.27 |
| 180 | 47.6 | 44.2 | 37 | 28.7 |
| 181 | 34.7 | 14.5 | 14 | 9.13 |

| | | | | |
|---|---|---|---|---|
| 182 | 9.36 | 0 | 0 | 0 |
| 183 | 30.1 | 12.6 | 11.9 | 0 |
| 184 | 20.6 | 14.6 | 14.6 | −10,000 |
| 185 | 45.7 | 39.8 | 34.8 | 21.4 |
| 186 | 11.9 | 12.5 | 12.1 | 0 |
| 187 | 6.66 | 9.04 | 8.46 | 0 |
| 188 | 10 | 9.97 | 9.97 | −10,000 |
| 189 | 20.7 | 19.5 | 18.4 | 12.3 |
| 190 | 29.8 | 18.3 | 18.3 | −10,000 |
| 191 | 20 | 12.9 | 12.5 | 0 |
| 192 | 22.5 | 10.3 | 10.1 | 0 |
| 193 | 55 | 31.7 | 31.2 | 9.85 |
| 194 | 24.8 | 9.89 | 9.89 | −10,000 |
| 195 | 7.95 | 10.9 | 10.7 | 4.71 |
| 196 | 14 | 5.64 | 5.64 | −10,000 |
| 197 | 24.6 | 9.32 | 9.32 | −10,000 |
| 198 | 54.4 | 56.7 | 47.1 | 38.4 |
| 199 | 33.8 | 20.9 | 20 | 6.84 |
| 200 | 22 | 16.4 | 16.1 | 4.3 |
| 201 | 26.2 | 14.1 | 13.8 | 3.7 |
| 202 | 75.8 | 30 | 28.3 | 13.9 |
| 203 | 14.9 | 11 | 10.7 | 0 |
| 204 | 27.5 | 28.6 | 25.2 | 17.7 |
| 205 | 12.3 | 12.4 | 12.1 | 0 |
| 206 | 6.18 | 6.8 | 6.8 | −10,000 |
| 207 | 55.7 | 35 | 32.1 | 19.1 |
| 208 | 11.6 | 10.2 | 10.2 | −10,000 |
| 209 | 27.6 | 10.9 | 10.4 | 4.89 |
| 210 | 17.6 | 10.6 | 10.6 | −10,000 |
| 211 | 26 | 17.1 | 16.5 | 8.7 |
| 212 | 22.6 | 14 | 14 | −10,000 |
| 213 | 32.6 | 15.2 | 14.8 | 8.61 |
| 214 | 36.6 | 22.2 | 22.2 | −10,000 |
| 215 | −10,000 | −10,000 | −10,000 | −10,000 |
| 216 | 54.6 | 29.9 | 29.9 | −10,000 |
| 217 | 43 | 17.2 | 17.2 | −10,000 |
| 218 | 45 | 22.4 | 22.4 | −10,000 |
| 219 | 24.6 | 22.2 | 22.2 | −10,000 |
| 220 | 53.1 | 17.1 | 16.8 | 5.29 |
| 221 | 29.6 | 14.6 | 14.6 | −10,000 |
| 222 | 12.5 | 11.9 | 11.9 | −10,000 |
| 223 | 40.7 | 16.2 | 16.2 | −10,000 |
| 224 | 39.5 | 18.9 | 18.9 | −10,000 |
| 225 | 36.2 | 19.6 | 19.6 | −10,000 |
| 226 | 62.6 | 36.9 | 36.8 | 0 |
| 227 | 68.4 | 21 | 21 | −10,000 |
| 228 | 12.1 | 13.3 | 13.3 | −10,000 |
| 229 | 43.8 | 25.4 | 25.4 | −10,000 |
| 230 | 34.6 | 18.3 | 18.3 | −10,000 |
| 231 | 28 | 14.8 | 14.8 | −10,000 |
| 232 | 47.5 | 16.2 | 16.2 | −10,000 |
| 233 | 21.4 | 11.1 | 11.1 | −10,000 |
| 234 | 20.2 | 13.2 | 13.2 | −10,000 |
| 235 | 20.7 | 13.8 | 13.8 | −10,000 |
| 236 | 29.5 | 16.1 | 16.1 | −10,000 |
| 237 | 35.1 | 14.8 | 14.8 | −10,000 |

| | | | | |
|---|---|---|---|---|
| 238 | 48.2 | 21 | 21 | −10,000 |
| 239 | −10,000 | −10,000 | −10,000 | −10,000 |
| 240 | −10,000 | −10,000 | −10,000 | −10,000 |
| 241 | 16.5 | 12.5 | 12.5 | −10,000 |
| 242 | 27.6 | 20.2 | 20.6 | 13.6 |
| 243 | 41.7 | 19.4 | 19.4 | −10,000 |
| 244 | 40.1 | 27.2 | 27.2 | −10,000 |
| 245 | 33.7 | 20.2 | 20.2 | −10,000 |
| 246 | 54.1 | 29.2 | 29.2 | 8.85 |
| 247 | 27.5 | 19.4 | 19.4 | −10,000 |
| 248 | 11.9 | 8.72 | 8.72 | −10,000 |
| 249 | 37.3 | 22.2 | 22.2 | −10,000 |
| 250 | 36.9 | 15.5 | 15.5 | −10,000 |
| 251 | 26 | 19.7 | 19.7 | −10,000 |
| 252 | 45.1 | 28.4 | 26.4 | 17 |
| 253 | 49.1 | 27 | 26.9 | 2.27 |

Cell number <4 = Patients with less than 4 voxels. Cell number −10,000 = No radiomic features calculated due to absence of corresponding masks.

**Table S2.** Estimated number of features used in model fitting after feature selection was performed.

| | **Full** | **Corr** | **Lincomb** | **PCA** |
|---|---|---|---|---|
| **Whole Tumor and Edema Masks** | | | | |
| All features | 1070 | 120 | 250 | 25 |
| Individual Sequences | 214 | 77 | 210 | 22 |
| CE without edema | 107 | 36 | 105 | 12 |
| **Necrotic, Enhancing, and Edema Masks** | | | | |
| All features | 1605 | 190 | 250 | 35 |
| Individual Sequences | 321 | 115 | 248 | 30 |
| CE without edema | 214 | 73 | 210 | 22 |

Note: Estimates for the high correlation filter, linear combinations filter, and PCA may vary between different cross validated split of data and when applied to the individual sequences may vary depending on which sequence was used. CE: Contrast enhanced; Full: full feature set; corr: high correlation filter; Lincomb: linear combinations filter; PCA: Principal component analysis.

**Table S3.** Predictive performance of the top 10 models in terms of mean cross-validated Brier Score and AUC for models across all sequences.

| Rank | Whole Tumor and Edema Masks (First Pipeline) | | | | Necrotic, Enhancing, and Edema Masks (Second Pipeline) | | | |
|---|---|---|---|---|---|---|---|---|
| | **Model** | **Feature Selection** | **Brier Score Mean (95% CI)** | **Accuracy Mean (95% CI)** | **Model** | **Feature Selection** | **Brier Score Mean (95% CI)** | **Accuracy Mean (95% CI)** |
| **1** | gbrm | full | 0.370 (0.236, 0.460) | 0.732 (0.627, 0.824) | gbrm | corr | 0.325 (0.232, 0.488) | 0.771 (0.608, 0.843) |
| **2** | svmRad | full | 0.374 (0.310, 0.460) | 0.727 (0.647, 0.824) | gbrm | full | 0.334 (0.215, 0.434) | 0.776 (0.700, 0.880) |
| **3** | svmPoly | full | 0.377 (0.302, 0.451) | 0.745 (0.686, 0.843) | rf | corr | 0.337 (0.269, 0.455) | 0.785 (0.686, 0.880) |
| **4** | gbrm | corr | 0.379 (0.254, 0.482) | 0.733 (0.627, 0.824) | rf | full | 0.351 (0.278, 0.466) | 0.759 (0.627, 0.920) |
| **5** | rf | full | 0.383 (0.306, 0.453) | 0.722 (0.647, 0.804) | svmRad | full | 0.355 (0.259, 0.468) | 0.753 (0.667, 0.843) |
| **6** | rf | corr | 0.383 (0.299, 0.459) | 0.730 (0.620, 0.824) | svmRad | pca | 0.365 (0.273, 0.461) | 0.732 (0.647, 0.824) |
| **7** | enet | full | 0.387 (0.284, 0.458) | 0.727 (0.588, 0.843) | ridge | pca | 0.366 (0.290, 0.455) | 0.741 (0.647, 0.880) |
| **8** | lasso | full | 0.388 (0.286, 0.454) | 0.728 (0.620, 0.824) | enet | pca | 0.367 (0.274, 0.481) | 0.734 (0.667, 0.804) |
| **9** | ridge | full | 0.390 (0.257, 0.480) | 0.729 (0.660, 0.863) | ada | full | 0.369 (0.274, 0.479) | 0.760 (0.647, 0.804) |
| **10** | ridge | pca | 0.397 (0.288, 0.488) | 0.73 (0.647, 0.863) | ada | corr | 0.37 (0.325, 0.421) | 0.764 (0.608, 0.840) |

gbrm—generalized boosted regression model; svmRad—SVM with a radial kernel; svmPoly—support vector machine (SVM) with a polynomial kernel; Enet—elastic net; rf–random forest; lasso—least absolute shrinkage and selection operator; ada—adaboost; full—full feature set; corr—high correlation filter; pca—principal component analysis.

**Table S4.** Predictive performance of the top 10 models in terms of mean cross-validated Brier Score and AUC for models across individual sequences.

| Rank | Whole Tumor and Edema Masks (First Pipeline) | | | | | Necrotic, Enhancing and Edema Masks (Second Pipeline) | | | | |
|---|---|---|---|---|---|---|---|---|---|---|
| | Seq | Model | Feature Selection | Brier Score Mean (95% CI) | Accuracy Mean (95% CI) | Seq | Model | Feature Selection | Brier Score Mean (95% CI) | Accuracy Mean (95% CI) |
| **1** | CE | gbrm | full | 0.361 (0.222, 0.528) | 0.756 (0.660, 0.863) | CE | gbrm | full | 0.311 (0.223, 0.466) | 0.796 (0.667, 0.880) |
| **2** | CE | gbrm | lincomb | 0.361 (0.237, 0.486) | 0.750 (0.640, 0.824) | CE | gbrm | corr | 0.324 (0.229, 0.430) | 0.791 (0.686, 0.860) |
| **3** | CE | nnet | lincomb | 0.366 (0.279, 0.463) | 0.746 (0.640, 0.863) | CE | rf | corr | 0.327 (0.265, 0.451) | 0.798 (0.686, 0.900) |
| **4** | CE | rf | corr | 0.367 (0.288, 0.460) | 0.740 (0.640, 0.824) | CE | gbrm | lincomb | 0.338 (0.225, 0.541) | 0.780 (0.686, 0.902) |
| **5** | CE | rf | lincomb | 0.368 (0.288, 0.470) | 0.749 (0.608, 0.863) | T1 | gbrm | full | 0.340 (0.231, 0.463) | 0.771 (0.680, 0.900) |
| **6** | CE | rf | full | 0.369 (0.302, 0.472) | 0.753 (0.627, 0.863) | T2 | gbrm | corr | 0.340 (0.224, 0.506) | 0.772 (0.608, 0.863) |
| **7** | CE | svmRad | lincomb | 0.372 (0.294, 0.487) | 0.726 (0.640, 0.863) | CE | svmRad | pca | 0.340 (0.253, 0.443) | 0.769 (0.627, 0.860) |
| **8** | CE | svmRad | full | 0.372 (0.286, 0.495) | 0.726 (0.640, 0.863) | CE | rf | full | 0.341 (0.268, 0.461) | 0.760 (0.608, 0.860) |
| 9 | CE | enet | full | 0.373 (0.301, 0.491) | 0.743 (0.647, 0.820) | CE | nnet | pca | 0.341 (0.251, 0.427) | 0.779 (0.667, 0.860) |
| 10 | CE | svmPoly | full | 0.378 (0.296, 0.481) | 0.720 (0.647, 0.824) | T2 | rf | corr | 0.342 (0.242, 0.514) | 0.771 (0.686, 0.860) |

CE—T1 contrast enhanced; gbrm—generalized boosted regression model; nnet—neural network; rf—random forest; svmRad—SVM with a radial kernel; enet—elastic net; svmPoly—support vector machine (SVM) with a polynomial kernel; full—full feature set; lincomb—linear combinations filter; corr—high correlation filter; pca—principal component analysis.

**Table S5.** Predictive performance of the top 10 models in terms of mean cross-validated Brier Score and AUC for models on T1 CE sequence without edema mask.

| Models Fit Only to CE Sequence without Edema Masks | | | | | | | | |
|---|---|---|---|---|---|---|---|---|
| **Rank** | **Whole Tumor Mask** | | | | **Necrotic and Enhancing Masks** | | | |
| | **Model** | **Feature Selection** | **Brier Score Mean (95% CI)** | **Accuracy Mean (95% CI)** | **Model** | **Feature Selection** | **Brier Score Mean (95% CI)** | **Accuracy Mean (95% CI)** |
| **1** | rf | corr | 0.357 (0.262, 0.443) | 0.752 (0.620, 0.843) | svmRad | pca | 0.325 (0.255, 0.485) | 0.782 (0.686, 0.860) |
| **2** | rf | lincomb | 0.364 (0.276, 0.490) | 0.759 (0.640, 0.863) | rf | corr | 0.327 (0.261, 0.458) | 0.791 (0.667, 0.880) |
| **3** | svmRad | corr | 0.365 (0.244, 0.460) | 0.749 (0.627, 0.843) | gbrm | full | 0.329 (0.230, 0.473) | 0.787 (0.725, 0.863) |
| **4** | rf | full | 0.365 (0.273, 0.492) | 0.756 (0.627, 0.882) | gbrm | lincomb | 0.330 (0.219, 0.446) | 0.775 (0.706, 0.843) |
| **5** | nnet | lincomb | 0.367 (0.319, 0.442) | 0.759 (0.660, 0.824) | svmRad | corr | 0.331 (0.237, 0.425) | 0.767 (0.680, 0.863) |
| **6** | svmRad | full | 0.367 (0.258, 0.477) | 0.757 (0.627, 0.882) | svmRad | full | 0.342 (0.269, 0.443) | 0.764 (0.667, 0.843) |
| **7** | nnet | pca | 0.369 (0.239, 0.450) | 0.750 (0.620, 0.863) | svmRad | lincomb | 0.343 (0.263, 0.436) | 0.764 (0.667, 0.843) |
| **8** | gbrm | lincomb | 0.370 (0.296, 0.478) | 0.761 (0.640, 0.843) | gbrm | corr | 0.343 (0.237, 0.528) | 0.777 (0.667, 0.863) |
| **9** | svmRad | pca | 0.371 (0.266, 0.468) | 0.750 (0.667, 0.863) | rf | full | 0.346 (0.263, 0.498) | 0.764 (0.627, 0.860) |
| **10** | svmPoly | lincomb | 0.371 (0.233, 0.471) | 0.745 (0.667, 0.863) | enet | full | 0.351 (0.267, 0.454) | 0.761 (0.667, 0.824) |

rf—random forest; svmRad—SVM with a radial kernel; nnet—neural network; gbrm—generalized boosted regression model; svmPoly—support vector machine (SVM) with a polynomial kernel; Enet—elastic net; corr—high correlation filter; lincomb—linear combinations filter; full—full feature set; pca—principal component analysis.

**Table S6.** Feature importance for the highest performing models.

| Using All (Multiparametric MRI) Sequences | | | | | | |
|---|---|---|---|---|---|---|
| | **GBRM Full—Whole Tumor (WT) and Edema Masks** | | | **GBRM Corr—Necrotic, Enhancing and Edema Masks** | | |
| **Rank** | **Seq** | **Mask** | **Variable** | **Seq** | **Mask** | **Variable** |
| 1 | T2 | WT | firstorder_Energy | CE | Nec | ngtdm_Coarseness |
| 2 | CE | WT | firstorder_10Percentile | CE | Enh | ngtdm_Busyness |
| 3 | A | WT | gldm_DependenceNonUniformity | T2 | Enh | ngtdm_Busyness |
| 4 | T1 | WT | glszm_LargeAreaEmphasis | F | Enh | glcm_ClusterShade |
| 5 | A | WT | glszm_LargeAreaHighGrayLevelEmphasis | T2 | Enh | shape_Sphericity |
| 6 | CE | WT | glrlm_RunLengthNonUniformity | T2 | Nec | shape_Sphericity |
| 7 | T2 | WT | ngtdm_Busyness | F | Nec | ngtdm_Coarseness |
| 8 | T1 | WT | firstorder_Skewness | T1 | Enh | glszm_SmallAreaLowGrayLevelEmphasis |
| 9 | F | WT | glcm_ClusterShade | T2 | Enh | glcm_Imc1 |
| 10 | T2 | WT | glcm_JointAverage | T1 | Enh | firstorder_Skewness |
| **Using Individual T1 CE Sequence** | | | | | | |
| | **GBRM Full—Whole Tumor (WT) and Edema Masks** | | | **GBRM Full—Necrotic, Enhancing and Edema Masks** | | |
| **Rank** | **Seq** | **Mask** | **Variable** | **Seq** | **Mask** | **Variable** |
| 1 | CE | WT | shape_Maximum2DDiameterRow | CE | Nec | ngtdm_Coarseness |
| 2 | CE | WT | shape_MeshVolume | CE | Enh | shape_MajorAxisLength |
| 3 | CE | WT | shape_Maximum2DDiameterColumn | CE | Enh | shape_Maximum2DDiameterRow |
| 4 | CE | WT | shape_Maximum2DDiameterSlice | CE | Enh | shape_SurfaceArea |
| 5 | CE | WT | firstorder_Skewness | CE | Enh | shape_Maximum2DDiameterSlice |
| 6 | CE | WT | ngtdm_Strength | CE | Enh | shape_Sphericity |
| 7 | CE | WT | firstorder_10Percentile | CE | Enh | ngtdm_Coarseness |
| 8 | CE | WT | glrlm_RunLengthNonUniformity | CE | Enh | shape_SurfaceVolumeRatio |

| | | | | | | |
|---|---|---|---|---|---|---|
| 9 | CE | WT | shape_MajorAxisLength | CE | Enh | firstorder_Median |
| 10 | CE | WT | shape_Sphericity | CE | Enh | firstorder_Kurtosis |
| **Using T1 CE Sequence without Edema Mask** | | | | | | |
| | | **RF Corr—Whole Tumor (WT) Mask** | | **RF Corr—Necrotic and Enhancing Masks** | | |
| **Rank** | **Seq** | **Mask** | **Variable** | **Seq** | **Mask** | **Variable** |
| 1 | CE | WT | gldm_DependenceNonUniformity | CE | Enh | gldm_DependenceNonUniformity |
| 2 | CE | WT | ngtdm_Coarseness | CE | Nec | ngtdm_Coarseness |
| 3 | CE | WT | firstorder_10Percentile | CE | Enh | ngtdm_Coarseness |
| 4 | CE | WT | firstorder_Skewness | CE | Nec | shape_Sphericity |
| 5 | CE | WT | glszm_LargeAreaHighGrayLevelEmphasis | CE | Enh | shape_Sphericity |
| 6 | CE | WT | glszm_ZoneVariance | CE | Enh | firstorder_10Percentile |
| 7 | CE | WT | glcm_Correlation | CE | Enh | shape_Flatness |
| 8 | CE | WT | ngtdm_Busyness | CE | Enh | ngtdm_Busyness |
| 9 | CE | WT | ngtdm_Strength | CE | Enh | shape_Flatness |
| 10 | CE | WT | shape_Sphericity | CE | Enh | firstorder_Minimum |

CE—T1 contrast enhanced; WT—whole tumor mask; Enh—enhancing mask; Nec—necrotic mask; gbrm—generalized boosted regression model; rf—random forest; corr—high correlation filter; full—full feature set.